Poly(hydroxybutyrate) in Vivo: NMR and X-ray Characterization of the Elastomeric State

Stuart R. Amor, Trevor Rayment, and Jeremy K. M. Sanders*

University Chemical Laboratory, Lensfield Road, Cambridge CB2 1EW, United Kingdom

Received October 25, 1990; Revised Manuscript Received March 21, 1991

ABSTRACT: Variable-temperature ^{13}C NMR relaxation studies of whole cells of *Alcaligenes eutrophus* show that poly(β-hydroxybutyrate) (PHB) is an amorphous elastomer in its "native" state within granules. The in vivo T_g is estimated be around −40 °C. Rotational correlation times and Arrhenius and other kinetic parameters are all consistent with amorphous elastomers that have been well characterized as bulk polymers. X-ray powder diffraction patterns of whole cells confirm that essentially 100% of PHB in its native state is amorphous.

Introduction

Poly(hydroxybutyrate) (PHB, 1) is a microbial storage polymer with intriguing properties. The isolated material

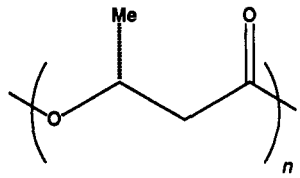

1

is highly crystalline, melting at 173–180 °C, and with a glass transition temperature (T_g) of 9 °C,[1] but in the live cell it is found in discrete granules whose physical properties have been the subject of much discussion. Electron microscopy[2] and CPMAS[3,4] NMR studies of isolated and dried granules indicated the presence of highly crystalline structures, which were assumed to be present also in native granules. This interpretation, while apparently providing a satisfactory physical description of granule structure, created a problem in understanding how the depolymerase enzyme could work so efficiently on a solid crystalline substrate. This conflict remained unsolved for many years.

Recent work in this laboratory[5,6] showed that, contrary to earlier belief, PHB is in a predominantly "mobile" state within the granules. Our conclusion was based on the observation of high-resolution ^{13}C NMR spectra of PHB using solution techniques on live cells of *Alcaligenes eutrophus* and two *Methylobacterium* species. The frequency of local molecular motions required to give such sharp resonances are of the order of 10^7 s^{-1}. The ^{13}C NMR properties over the temperature range 10–30 °C matched qualitatively those expected of an amorphous polymer above its T_g: the observed small NOE for main-chain carbons, longer T_1s at lower temperatures, and dramatic broadening of the signals over a small temperature range are well-documented features of such elastomeric polymers.[7] We also showed that treatments of the kind used to prepare isolated granules for spectroscopy can lead to solidification of the PHB to give the crystalline structures previously observed.

We now report detailed ^{13}C NMR measurements of PHB in its native state over a much larger temperature range and at two different field strengths. By fitting the relaxation parameters to a detailed model and comparison with well-characterized bulk synthetic polymers, we show that the physical properties of PHB in submicron granules are consistent with those of a bulk elastomer with T_g of around −40 °C. Furthermore we have used X-ray powder diffraction of whole cells to demonstrate the absence of significant amounts of crystalline material. We shall discuss elsewhere the mechanism of PHB plasticization in vivo.

Theory

We consider only amorphous polymers well above their T_g; molecular motion in such materials is sufficiently fast to give sharp spectra by averaging carbon–proton dipolar couplings and chemical shift anisotropies. Below T_g, molecular motion even in amorphous regions is too slow. Then solid-state NMR techniques such as CPMAS have to be used.[7]

Relaxation studies[7] of amorphous elastomers above T_g generally assume that, in common with isotropic rotational diffusion in solution, the correlation time associated with the motion of the CH vector (τ_c) is dependent on temperature and follows an Arrhenius relationship:

$$\tau_c = \tau_c^\circ \exp(-E_a/RT) \quad (1)$$

where E_a is an activation energy for the rotation. The various models of polymer motion and the above assumption are used to predict how the relaxation parameter should vary with temperature. The predicted curves are fitted to the relaxation data by varying the parameters of the model, the preexponential factor (τ_c°), and E_a. We have proceeded in a slightly different manner. We have assumed a simple model from which, given a T_1 value, we can obtain an estimate of τ_c. Plots of ln τ_c against inverse temperature have allowed the calculation of a value for the activation energy of the barrier to the motion causing T_1 relaxation and this has been compared to those found for bulk synthetic elastomers.

Assuming that carbon relaxation occurs purely by the ^{13}C–^1H dipolar relaxation mechanism, the spin–lattice relaxation time (T_1), the spin–spin relaxation time (T_2) and NOE are given by the well-known expressions[8]

$$\frac{1}{T_1} = \frac{h^2\gamma_C^2\gamma_H^2}{40\pi^2}\sum_i r_i^{-6}[J(\omega_H - \omega_C) + 3J(\omega_C) + 6J(\omega_H + \omega_C)] \quad (2)$$

0024-9297/91/2224-4583$02.50/0

$$\frac{1}{T_2} = \frac{1}{2T_1} + \frac{h^2\gamma_C^2\gamma_H^2}{80\pi^2}\sum_i r_i^{-6}[4J(0) + 6J(\omega_H)] \quad (3)$$

$$\mathrm{NOE} = 1 + \frac{\gamma_H}{\gamma_C}\left[\frac{6J(\omega_H + \omega_C) - J(\omega_H - \omega_C)}{J(\omega_H - \omega_C) + 3J(\omega_C) + 6J(\omega_H + \omega_C)}\right] \quad (4)$$

where γ_C and γ_H are the carbon and proton gyromagnetic ratios, respectively; ω_C and ω_H are the corresponding resonance frequencies, r_i is the distance between the ^{13}C nucleus of interest and the ith relaxing proton, and $J(\omega_i)$ is the spectral density function. Normally for T_1 measurements, only directly bonded protons (with bond length r_{CH}) are considered—the r^{-6} dependence of dipole–dipole interactions ensures that their influence far outweighs any other protons. Therefore, ^{13}C T_1s are roughly proportional to the inverse of the number of bound protons for a given value of τ_c. The spectral density functions are Fourier transforms of the autocorrelation functions of second-order spherical harmonics. They describe the power available at angular frequency ω_i from the fluctuating interaction. The form of $J(\omega_i)$ depends on the model used to describe the molecular motion.

The simplest model generally used is that of isotropic rotational diffusion, where $J(\omega_i)$ has the following form:

$$J(\omega_i) = \tau_c/(1 + \omega_i^2\tau_c^2) \quad (5)$$

A major drawback of the simple isotropic model with respect to polymers is its inability to predict correctly the value of the T_1 minimum. More complicated models incorporating segmental motions involving several,[9] or a distribution of, correlation times[10] or librational motions[11] have been invoked to account for the discrepancies between the experimental T_1s and those predicted by the isotropic model. All these models incorporate longer correlation times to account for the observation of smaller NOEs and larger line widths than expected at high temperatures. For example, Howarth[12] measured the temperature dependence of ^{13}C T_1s and NOEs for natural rubber. He argued that the ^{13}C T_1s could not be fitted simultaneously to experimental values at both the T_1 minimum and high temperature by use of models involving only isotropic reorientations. The data were, however, consistent with a three-correlation-time model or a combined fast anisotropic libration and reptation (looping motion) model. The three-correlation-time model involved a relatively slow isotropic motion, a slightly faster anisotropic motion, considered as a libration, and a fast anisotropic libration.

Dejean et al.[13] combined the conformational jump model of Hall and Helfand[9] with fast anisotropic librations to model accurately the ^{13}C T_1 variation of poly(vinyl methyl ether) with temperature at 62 and 25 MHz. We have adopted their approach as it is relatively simple and allows comparisons to be made both with the relaxation behavior of other amorphous elastomers and with PHB in tetrachloroethane solution.[14] The real part (Re) of the spectral density function for the Hall–Helfand (HH) model can be written as

$$J(\omega) = \mathrm{Re}\,[1/[(\alpha + i\beta)^{1/2}]] \quad (6)$$

where $\alpha = \tau_2^{-2} + 2\tau_1^{-1}\tau_2^{-1} - \omega^2$, $\beta = -2\omega(\tau_1^{-1} + \tau_2^{-1})$. τ_1 is the correlation time for the cooperative or correlated jumps responsible for orientation diffusion along the chain and τ_2 corresponds to damping either by nonpropagative specific single conformational transitions or by distortions of the chain with respect to its most stable conformation. The correlation times, τ_1 and τ_2, can have different activation energies, which are associated with their different motions.

Dejean et al.[13] made the simplifying approximation that the ratio τ_2/τ_1 remains constant, in effect giving τ_2 and τ_1 the same activation energy but a different preexponential constant. For ratios τ_2/τ_1 between 2 and 10, this model gives T_1 values slightly different from the isotropic model for a given τ_1. For τ_2/τ_1 greater than 10, the HH model diverges significantly from the isotropic model only at correlation times shorter than 10^{-9} s, giving lower values of ^{13}C T_1 for a given τ_1. The value of τ_2/τ_1 was found to be invariant when values of T_1 were fitted against temperature for poly(vinyl methyl ether) in the bulk amorphous solid or in chloroform solution.[13] A recent study of PHB relaxation in tetrachloroethane solution using this approach gives an optimum τ_2/τ_1 ratio of around 3.[14]

A fast anisotropic libration causes the value of the T_1 minimum to be increased by an amount dependent on the angle of libration. The spectral density of a model combining the HH model and fast anisotropic bond librations can be written[13] as

$$J(\omega) = \frac{1-a}{(\alpha + i\beta)^{1/2}} + \frac{a\tau_0}{(1 + \omega^2\tau_0^2)} \quad (7)$$

so long as $\tau_0 \ll \tau_1$; where $\alpha = \tau_2^{-2} + 2\tau_1^{-1}\tau_2^{-1} - \omega^2$, $\beta = -2\omega(\tau_1^{-1} + \tau_2^{-1})$, τ_1 and τ_2 have the same physical meaning as above, τ_0 is the correlation time associated with the libration motion, and $(1 - a)^{1/2} = (\cos\theta - \cos^3\theta)/(2 - 2\cos\theta)$, where θ is the conic half-angle for libration. Designating

$$J_{HH}(\omega) = 1/[(\alpha + i\beta)^{1/2}]$$

and

$$J_0(\omega) = \tau_0/(1 + \omega^2\tau_0^2)$$

this allows T_1^{-1} to be written as the sum of two terms:

$$\frac{1}{T_1} = (1-a)\frac{h^2\gamma_C^2\gamma_H^2}{40\pi^2}r_{CH}^{-6}[J_{HH}(\omega_H - \omega_C) + 3J_{HH}(\omega_C) + 6J_{HH}(\omega_H + \omega_C)] + a\frac{h^2\gamma_C^2\gamma_H^2}{40\pi^2}r_{CH}^{-6}[J_0(\omega_H - \omega_C) + 3J_0(\omega_C) + 6J_0(\omega_H + \omega_C)] \quad (8)$$

If $(\omega_H + \omega_C)\tau_0 \ll 1$, then the second term can be neglected and T_1 is lengthened by a factor of $1/(1 - a)$.

Howarth[12] and Dejean et al.[13] set $(1 - a)$ so that the theoretical T_1 matches the experimental T_1; the value of θ can then be calculated by solving the cubic equation in $\cos\theta$. Dejean et al. set the ratio τ_1/τ_0 to be constant and sufficiently large that $(\omega_H + \omega_C)\tau_0 \ll 1$ throughout the temperature range. The second term of the above equation can be neglected, and the T_1 minimum is then approximately equal to the T_1 minimum of the HH model multiplied by $1/(1 - a)$. This assumes that the activation energy of libration motion is the same as that for the τ_1 motion. While it seems likely that τ_1 and τ_2 have activation energies of the same order (For PHB in tetrachloroethane solution, E_a for τ_1 and τ_2 are 22 and 42 kJ mol^{-1}, respectively.), it appears unlikely that E_a for the libration will be the same also. Howarth noted that wide variation in his fast libration correlation time had little effect on the relaxation parameters and set it to a fixed value.[11]

If the correlation time τ_1 follows an Arrhenius relationship, then a plot of ln τ_1 against inverse temperature should yield a straight line whose gradient is $-E_a/R$. On the other hand, τ_1 in bulk polymers tends to follow the

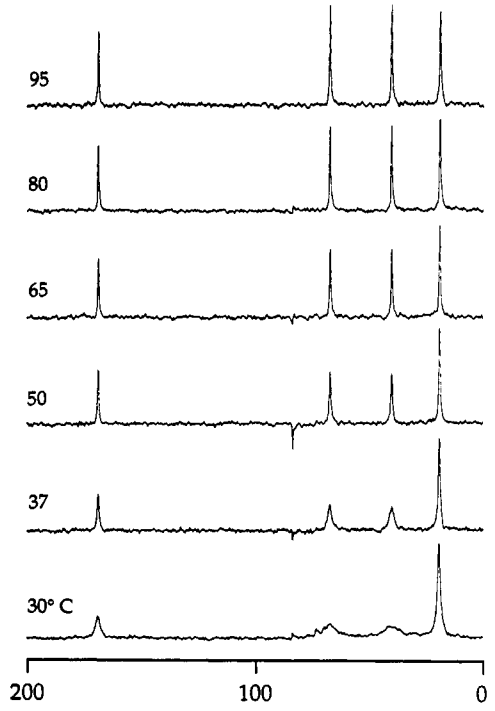

Figure 1. 100-MHz natural-abundance ^{13}C spectra of suspensions of *A. eutrophus* cells at various temperatures. Each spectrum is the result of acquiring 200 transients.

Williams–Landel–Ferry (WLF) equation.[15] This empirical relationship gives the ratio of the τ_1 at a temperature T to that of a reference temperature (usually taken as T_g) for a polymer in the range T_g to around $T_g + 100$:

$$\log\left(\frac{\tau_C(T)}{\tau_C(T_{ref})}\right) = \frac{-C_1(T - T_{ref})}{C_2 + (T - T_{ref})} \quad (9)$$

C_1 and C_2 are arbitrary factors that vary according to the reference temperature chosen. With $T_{ref} = T_g$, C_1 and C_2 were at first thought to be universal constants, but they have since been shown to vary slightly from polymer to polymer;[16] they fall in the small range 11–17 for C_1 and 40–70 for C_2 except for polyisobutylene, which has an abnormally high value of C_2. While it is obviously impossible for the correlation time simultaneously to satisfy both an Arrhenius ($1/T$) and WLF (T) dependence on temperature, experimental error and small temperature range available often preclude distinction between these two mathematical models. In common with others,[17] we will show that our data are consistent with both models.

Results and Discussion

Temperature Dependence of ^{13}C Spectra. Figure 1 shows 100-MHz proton-decoupled ^{13}C spectra of stationary-phase *A. eutrophus* cells over the temperature range 30–95 °C. Each spectrum is the result of collecting 200 transients; 10-s relaxation delays were allowed between acquisitions to ensure reliable peak intensities to be observed. The most striking features of this series of spectra are (a) that PHB is the only species detected, a measure of the huge internal concentration of mobile polymer within the cell, and (b) the variation in the relative heights of the carbon signals. All the temperature-dependent features of these spectra are fully reversible. While heat-treated cells are clearly not viable, there are no irreversible changes detected in the spectroscopic properties of the granules within these cells.

These variations are easily interpreted qualitatively. At 30 °C, the methyl carbon resonance is receiving almost its full NOE and is relatively sharp as a result of fast internal rotation about the methyl–methine bond. Only the much slower overall reorientation of the polymer backbone is available to the methylene and methine carbons, so their resonances are broad and lack the NOE. By 50 °C, faster backbone motion has dramatically sharpened the methylene and methine signals but not yet brought the NOE into action; the methyl carbon resonance is about twice the height of the other carbon signals. At 95 °C, the methylene and methine signals are roughly the same intensity as the methyl signal because faster overall reorientations of the polymer backbone at higher temperature have increased their NOEs substantially and sharpened the signals. These line-width results are summarized in Table I. Qualitatively similar results at 62.9 MHz are given in Table II.

Table I
Temperature Dependence of Line Widths of Native PHB at 100.1 MHz

	line width at 100.1 MHz, Hz			
temp, °C	CO	CH	CH_2	CH_3
30	250	>400	>400	110
37	100	220	280	70
50	50	65	70	40
65	35	35	40	30
80	30	30	30	30
95	30	30	30	30

Table II
Temperature Dependence of Line Widths of Native PHB at 62.9 MHz

	line width at 62.9 MHz, Hz			
temp, °C	CO	CH	CH_2	CH_3
30	80	>250	>250	70
40	25	40	45	15
50	15	20	25	10
65	15	15	25	10
80	15	15	15	10

Table III
Temperature Dependence of T_1 of Native PHB at 100.1 MHz

	T_1 at 100.1 MHz, s			
temp, °C	CO	CH	CH_2	CH_3
30	8.2	1.4	0.53	0.62
37	5.3	0.90	0.36	0.57
50	2.5	0.45	0.24	0.55
65	1.4	0.30	0.16	0.58
80	1.3	0.30	0.18	0.65
95	1.9	0.34	0.23	0.98

These results confirm our earlier observations and conclusions but do not allow quantitative comparison with well-characterized bulk polymers. For this we turned to relaxation times.

Temperature Dependence of ^{13}C Relaxation Times. Spin–lattice relaxation times were measured at 100 MHz by saturation–recovery over the temperature range 30–95 °C. The results are summarized in Table III and were used to fit the above model as described below. Subsequently, further experiments were carried out at 62.9 MHz to test our predictions of methylene and methine carbon relaxation rates; these experimental results are given in Table IV. It is clear that the backbone carbons pass through the T_1 minimum around 65 °C. It is also qualitatively clear that the methylene/methine relaxation rate ratio, which ranges from 1.5 to 2.6, is close to 2, as would be expected if their relaxation were induced by effectively the same molecular motion.

Table IV
Temperature Dependence of T_1 of Native PHB at 62.9 MHz

	T_1 at 62.9 MHz, s			
temp, °C	CO	CH	CH_2	CH_3
30		0.48	0.20	0.47
40	2.1	0.21	0.11	0.49
50	1.8	0.17	0.10	0.46
65	1.5	0.19	0.10	0.49
80	1.5	0.19	0.10	0.50
90	1.6	0.30	0.16	0.79

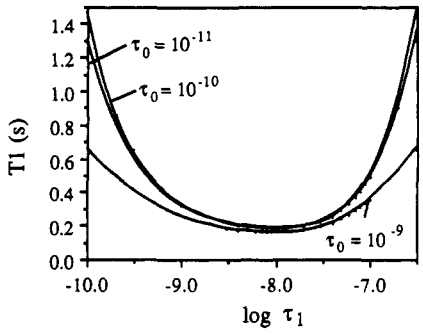

Figure 2. Calculated dependence of T_1 on τ_0 and τ_1.

The variation of the methyl T_1 is significantly different from the backbone carbons. The T_1 minimum is broader than those of the backbone carbons and is displaced to lower temperature because internal rotation is the major motion causing dipolar relaxation at low temperature. At high temperature this motion is too fast for efficient relaxation and the T_1 rapidly increases. We have not modeled the relaxation of this group as this would not add much to our understanding of the overall motional properties of PHB.

Modeling the Molecular Motion of Native PHB. At 95 °C the T_1s of the methine and methylene carbons have increased by less than 20% and 50%, respectively, of their minimum values. By use of the HH model and a value of 20 for the ratio τ_2/τ_1, the correlation time τ_1 varies between approximately 10^{-6} and 10^{-9} s. This is relatively insensitive to the τ_2/τ_1 ratio in this temperature range: with the HH model, the predicted ^{13}C T_1 at 100.1 MHz of the methine carbon is increased from 170 (isotropic model) to 210 ms (HH model; $\tau_2/\tau_1 = 20$). The experimental value is 300 ms, and no matter how large the τ_2/τ_1 ratio the Hall–Helfand model alone cannot predict a minimum that is this large.

Adding in the librational motions, we find (Figure 2) that variation of fixed τ_0 makes little difference to the T_1 relaxation around the T_1 minimum so long as $\tau_0 < 10^{-10}$. Therefore, we set τ_0 arbitrarily to 10^{-11} s and varied the value of $(1-a)$ so that the theoretical T_1 minimum matched the experimental minimum. The fixed parameters used for modeling ^{13}C T_1s of the methine and methylene carbons are $\tau_2/\tau_1 = 20$, $\tau_0 = 10^{-11}$ s, CH bond length 1.09 Å. For the methine carbon, the best fit at 100 MHz (Figure 3) was obtained with $(1-a) = 0.72$, and for the methylene carbon (Figure 4) $(1-a) = 0.67$. Calculation gives half-conic angles of libration of 26° and 29°, respectively, values that are very similar to the recent estimate of 22° and 29° for PHB in solution.[14] The lower value for methine carbons has been observed in many polymers and has been attributed to greater steric hindrance at the methine carbon.[12,13,18]

The predicted dependence of T_1 on log τ_1 at 100.1 MHz based on the above assumptions for both the methine and methylene carbons is given in Figure 5. The slightly different values for $(1-a)$ are reflected in the fact that

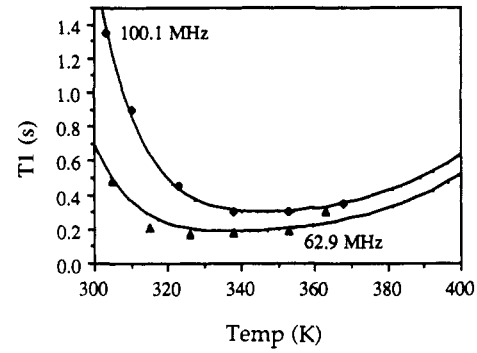

Figure 3. Temperature dependence of the methine carbon T_1 at 100 (●) and 62.9 MHz (▲). Curves are the best fit from the parameters given in the text.

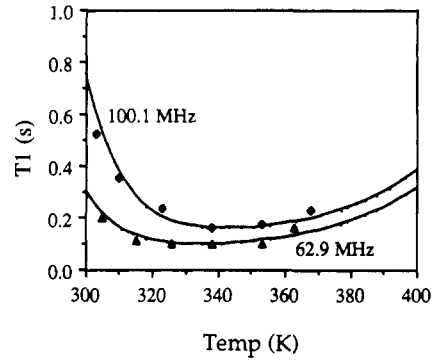

Figure 4. Temperature dependence of the methylene carbon T_1 at 100 (●) and 62.9 MHz (▲). Curves are the best fit from the parameters given in the text.

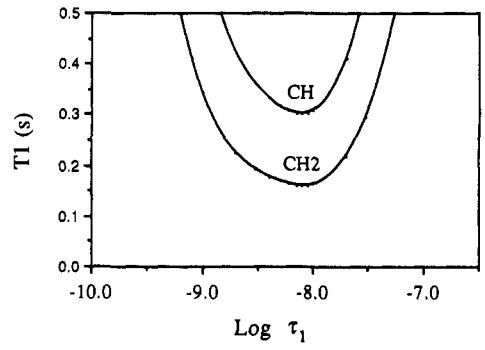

Figure 5. Predicted τ_1 dependence of methylene and methine carbon T_1 at 100 MHz from the best-fit parameters.

the ratio of methine T_1/methylene T_1 at the T_1 minimum is somewhat less than 2. Using the model outlined above (eq 8) and the values for the parameters τ_2/τ_1, $(1-a)$, and τ_0 obtained by fitting it to the experimental T_1s at 100.1 MHz, we predicted the ^{13}C T_1s of the methine and methylene carbon at 62.9 MHz as a function of temperature. This required also using the values for the preexponential term (τ_1^0) and E_a obtained from the Arrhenius plot (see below). The theoretical curves for the ^{13}C T_1s and experimental data for both methine and methylene groups are shown in Figures 3 and 4. The parameters and model give a prediction that fits all the T_1 data within experimental error.

Arrhenius Behavior. log τ_1 values at a particular temperature were obtained directly from comparison of the experimental T_1 values with the theoretical curves of Figure 5. The resulting Arrhenius plot is given in Figure 6 and show that, within experimental error, τ_1 does follow an Arrhenius relationship. The plots for both methine and methylene carbons yield activation energies that are essentially the same at $E_a = 57 \pm 5$ kJ mol^{-1}. The ratio

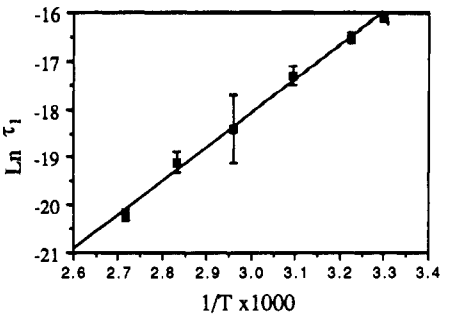

Figure 6. Arrhenius plot for the methine carbon.

Table V
Activation Energies for Motion of Bulk and Dissolved Polymers

polymer	E_{act} in soln, kJ mol^{-1}	E_{act} in bulk, kJ mol^{-1}
poly(vinyl methyl ether)[13]	15	39
poly(propylene oxide)[18]		49
poly(ethylene oxide)		49
PHB	19.5[14]	57[a]

[a] This work.

τ_2/τ_1 has little effect on the value of E_a: with $\tau_2/\tau_1 = 1$, $E_a = 52$ kJ mol^{-1}. This is of the same order as the reported activated energies of other amorphous polymers in bulk. Table V gives the literature values [13,14,18] for the activation energy of τ_1 for various polymers in bulk amorphous solid or in solution. The activation energy (E_a) can be thought of as being made up of two terms:[19]

$$E_a = E_\eta + E^* \tag{10}$$

where E_η is the activation energy required to overcome the viscosity of the solvent and E^* is the activation energy for the potential barrier of the local motion in the gas phase. Dais et al.[14] calculated that $E^* \approx 8$ kJ mol^{-1} for PHB in solution. Assuming the same value E^* for PHB in the native state, this gives $E_\eta \approx 50$ kJ mol^{-1} and confirms the importance of intermolecular interactions in bulk polymers found for poly(vinyl methyl ether).[13]

Williams–Landel–Ferry Behavior. In order to obtain values for the WLF constants we have estimated T_g by using the empirical relationship $T_c/T_g \approx 1.2$–1.3 found by Dekmezian,[17] where T_c is the lowest temperature at which high-resolution spectra can be obtained by solution techniques. Again polyisobutylene is an exception, with $T_c/T_g = 1.4$. Clearly T_c is dependent on the resonance observed (being lower for more mobile side-chain resonances than backbone resonances), the instrumentation involved, and the experimental procedure. However, a rough estimate is all that is required for the purpose of seeing if τ_1 obeys WLF kinetics. For PHB in its native state $T_c \approx 290$ K, which gives values of T_g in the range 220–240 K. We have used a value of $T_g = 230$ K to plot $(T - T_g)$ against $-(T - T_g)/\ln \tau_1$ for the methine carbon (Figure 7). This gives values of $C_1 = 12 \pm 1$ and $C_2 = 51 \pm 10$ (errors estimated by taking values of $T_g = 230 \pm 10$ K), which are clearly within the range found for most bulk amorphous polymers (Table VI).

X-ray Diffraction. The experiments above have shown that most native PHB is amorphous and mobile, but have not demonstrated the absence of crystalline material. However, the large weight fraction of PHB present even under in vivo conditions allows X-ray diffraction to be used to estimate the proportion of crystalline material.

Table VI
Values of C_1 and C_2 for Bulk Elastomers[17]

polymer	C_1	C_2
ethylene–propylene (62% Pr)	15.4	67.7
cis-polyisoprene	15.0	68.7
polyisobutylene	14.1	91.5
poly(vinyl acetate)	15.1	62.0
poly(isopropyl acrylate)	12.2	53.6
cis-polybutadiene	15.1	54.3
atactic polypropylene	15.2	60.7
native-state PHB[a]	12.0	51

[a] This work.

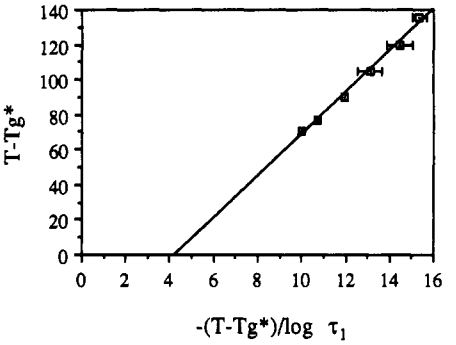

Figure 7. WLF plot for the methine carbon.

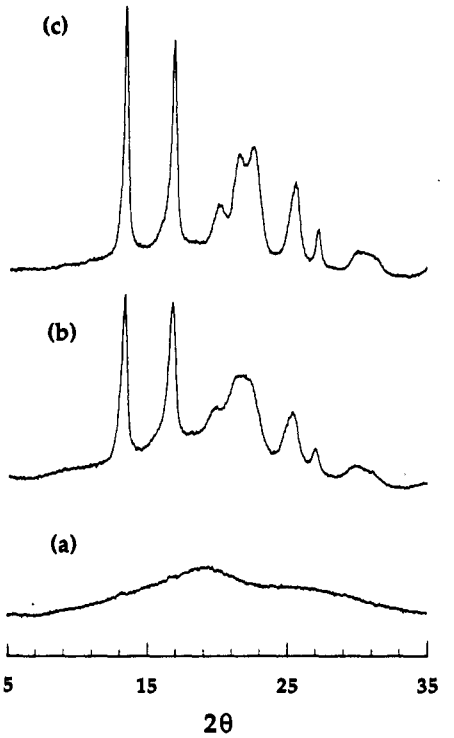

Figure 8. X-ray powder diffraction patterns for (a) a wet paste of *A. eutrophus* cells containing ca. 50% PHB by dry weight, (b) *A. eutrophus* cells that have been washed with acetone and dried (110 °C, 1 h), and (c) dry aqueously purified PHB.

Figure 8a shows that the X-ray powder diffraction pattern for a wet paste of *A. eutrophus* displays almost no features due to crystalline material. In contrast, when a sample of the same culture is washed in acetone and dried at 100 °C for 1 h a sharp diffraction pattern is observed (Figure 8b). This pattern is very similar to that of aqueously purified PHB (Figure 8c), whose crystal structure is well-known.[20]

We used the diffraction intensity to obtain quantitative estimates of crystallinity in these samples. In the diffraction pattern of "pure" PHB is seen a broad background

that arises from scattering by an amorphous component in the solid; the relative areas of the crystalline and amorphous diffraction patterns give an estimate of 65% crystallinity within this sample. In order to estimate the crystalline fraction of PHB within the wet-paste whole cells only the intensity of the strongest (020) reflections has been used, and absorption corrections have been made for the presence of water and other material. When these corrections have been made, a value of not more than 2% crystallinity is obtained, at the very limit of detection. If real, this crystallinity is probable produced by drying of cells at the surface of the sample. Thus in vivo X-ray diffraction shows that PHB in its native state is essentially all amorphous.[21]

Conclusions

We have shown that the relaxation behavior of PHB in its native state is typical of an amorphous elastomer above its T_g. Overall segmental molecular motion is the dominant cause of longitudinal relaxation, although the rate of such motion is much slower than in solution. The activation energy for the process causing T_1 relaxation in the native state is larger than for PHB in solution and is of the same magnitude as other bulk elastomers. Whole-cell X-ray diffraction shows that PHB in its native state is essentially all amorphous.

Strictly speaking, one cannot conclude that the model we have used, or any other model, necessarily elucidates the actual motions executed by the polymer chains. Any of the available models could probably be fitted to the methine and methylene ^{13}C T_1 data that we obtained from native-state PHB; nevertheless, it is noteworthy that the model we have used gives essentially the same values for librational excursions as is observed by Dais et al. for PHB in solution.[14]

The immediate aim of this work has been to show that the mobility and relaxation properties of native PHB match those of synthetic polymers, which can be studied in bulk. More generally, these experiments are a powerful illustration of the power of whole-cell NMR, allowing the bulk properties of the polymer to be obtained from submicron particles within a cell.

While these results give a good description of the PHB in native granules, they do not explain how bacteria are able to store a crystalline polymer as a mobile elastomer. We previously suggested that the PHB in the granules is plasticized by water.[6] Elsewhere we present evidence to support this idea and show that another plasticizing agent may also be required to explain the mobility.[22]

Experimental Section

Rich medium contained yeast extract (Oxoid L-21, 10 g/L), bacteriological peptone (Oxoid L-37, 10 g/L), Lab-lemco (Oxoid L-29, 5 g/L), fructose (10 g/L), and NaCl (5 g/L), pH 6.6. Minimal medium contained phosphate buffer (20 mL/L of stock NaH_2PO_4 (72 g/L), K_2HPO_4 (95 g/L)), ammonium sulfate (1.8 g/L), magnesium sulfate (0.2 g/L), and trace elements (6 mL/L of stock $CaCl_2$ (5.2 g/L), $CuSO_4 \cdot 5H_2O$ (0.08 g/L), $MnSO_4 \cdot 4H_2O$ (0.04 g/L), and $ZnSO_4 \cdot 7H_2O$ (0.04 g/L)). All media were sterilized by autoclaving for 20 min at 115 °C and 121 psi before use.

Alcaligenes eutrophus H16 (a naturally selected high-yielding strain supplied by ICI Biological Products, Billingham, UK) were grown on rich medium (500 mL) in 2-L shake flasks at 30 °C in an orbital incubator at 100 rpm. Cells were harvested when they reached an $O.D._{610}$ of approximately 1. They were then centrifuged at 4000*g* for 10 min and resuspended in minimal medium (500 mL) in 2-L shake flasks containing fructose (10 g/L) as the sole carbon source. They were incubated for 48 h at 100 rpm and 30 °C.

Bacteria were centrifuged for 10 min at 4000*g* and 4 °C. The soft pellet was washed and finally taken up in a minimal volume of isotonic saline. This suspension (0.5 mL) was placed in a 5-mm NMR tube. A sealed capillary of deuterated benzene or (above 70 °C) deuterated 1,2-tetrachloroethane in the center of the NMR tube acted as lock signal and chemical shift reference.

Carbon spectra at 100.1 and 62.9 MHz were taken on Bruker AM 400 and WH 250 spectrometers, respectively. Waltz-16 broad-band decoupling was used, the sweep width was 220 ppm, and 8192 data points were collected. A 90° pulse length was used and the delay time between pulses was 5 s. A total of 200 transients were collected.

T_1s of native PHB were measured by using saturation–recovery. The initial delay of the 90° pulse train was 200 ms; this was successively halved to ≈1 ms. Twelve interleaved variable delays, allowing T_1 relaxation, between 10 ms and 10 s were used. The same acquisition parameters as above were used and 64 transients were acquired. No relaxation delay between pulse sequences is required.

X-ray diffraction data were collected on a Philips PW1710 (θ–2θ) diffractometer using Cu Kα radiation (λ = 1.5418 Å). Samples were placed in a constant-volume sample holder, which allowed a determination of the density (ρ), and hence absorption coefficient, of the sample.

Acknowledgment. We are grateful to SERC, Pfizer, and ICI Biological Products for financial support and to Drs. B. K. Hunter and J. F. Stageman for valuable practical assistance and discussions.

References and Notes

(1) Mimoto, H.; Barham, P. J.; Keller, A. *Polym. Commun.* **1988**, *29*, 113.
(2) Ellar, D. J.; Lundgren, D. G.; Okamura, K.; Marchessault, R. H. *J. Mol. Biol.* **1968**, *35*, 489.
(3) Jacob, G. S.; Garbow, J. R.; Schaefer, J. *J. Biol. Chem.* **1986**, *261*, 16785.
(4) Doi, Y.; Kunioka, M.; Nakamura, Y.; Soga, K. *Makromol. Chem., Rapid Commun.* **1986**, *7*, 661.
(5) Barnard, G. N.; Sanders, J. K. M. *FEBS Lett.* **1988**, *231*, 16.
(6) Barnard, G. N.; Sanders, J. K. M. *J. Biol. Chem.* **1989**, *264*, 3286.
(7) Komoroski, R. A. *High Resolution NMR Spectroscopy of Synthetic Polymers in Bulk*; VCH: New York, 1986.
(8) Allerhand, A.; Doddrell, D.; Komoroski, R. A. *J. Chem. Phys.* **1971**, *55*, 189.
(9) Hall, C. K.; Helfand, E. *J. Chem. Phys.* **1982**, *77*, 3275.
(10) Schaefer, J. *Macromolecules* **1973**, *6*, 882.
(11) Jones, A. A.; Lubianez, R. P.; Hanson, M. A.; Shostak, S. L. *J. Polym. Sci., Polym. Phys. Ed.* **1978**, *16*, 1685.
(12) Howarth, O. W. *J. Chem. Soc., Faraday Trans. 2* **1980**, *76*, 1219.
(13) Dejean de la Batie, R.; Lauprêtre, Monnerie, L. *Macromolecules* **1988**, *21*, 2045.
(14) Dais, P.; Nedea, M. E.; Morin, F. G.; Marchessault, R. H. *Macromolecules* **1990**, *23*, 3387.
(15) Williams, M. L.; Landel, R. F.; Ferry, J. D. *J. Am. Chem. Soc.* **1955**, *77*, 3701.
(16) Ferry, J. D. *Viscoelastic Properties of Polymers*, 3rd ed.; Wiley: New York, 1980; Chapter 11.
(17) Dekmezian, A.; Axelson, D. E.; Dechter, J. J.; Borah, B.; Mandelkern, L. *J. Polym. Sci., Polym. Phys. Ed.* **1985**, *23*, 367.
(18) Dejean de la Batie, R.; Lauprêtre, Monnerie, L. *Macromolecules* **1988**, *21*, 2052.
(19) Tekeley, P.; Lauprêtre, F.; Monnerie, L. *Macromolecules* **1983**, *16*, 415.
(20) Yokouchi, M.; Chatani, Y.; Tadakoro, H.; Teranishi, K.; Tani, H. *Polymer* **197**, *14*, 267.
(21) Since submission of this manuscript, we have become aware of independent X-ray results similar to those reported here: Kawaguchi, Y.; Doi, Y. *FEMS Microbiol. Lett.* **1990**, *70*, 151.
(22) Harrison, S. T. L.; Amor, S. R.; Bonthrone, K. M.; Chase, H. A.; Sanders, J. K. M., submitted for publication.